

3
N80-19153

DEVELOPMENT OF ELECTROMAGNETIC ANALYSIS METHODS
FOR LARGE APERTURE ANTENNAS

C. R. Cockrell and L. D. Staton
NASA Langley Research Center

P. K. Agrawal*
RCA - Moorestown, N. J.

LSST 1ST ANNUAL TECHNICAL REVIEW

November 7-8, 1979

*Formerly with George Washington University at NASA Langley Research Center

173 INTENTIONALLY BLANK

OBJECTIVES

- TO ESTABLISH AND VERIFY TECHNIQUES FOR PREDICTION OF EM PERFORMANCE OF LARGE SPACE ANTENNAS
- TO DEVELOP STATISTICAL AND DETERMINISTIC MODELING TECHNIQUES- INCLUDING EFFECTS OF SURFACE ROUGHNESS, DISTORTION, AND SEGMENTATION

DESCRIPTION OF WORK

- EXTENSION OF PRESENT TECHNIQUES OF APERTURE INTEGRATION FOR LARGE, SEGMENTED REFLECTORS
 - ◆ Planar Segmentation
 - ◆ Curved Segmentation
- ANALYSES OF DETERMINISTICALLY DISTORTED LARGE REFLECTORS WHOSE SHAPE IS DETERMINED BY SAMPLED POINTS
- UNIFIED APPLICATION OF STATISTICAL CORRELATION THEORY FOR BOTH SURFACE ROUGHNESS AND LARGE SCALE SURFACE DEVIATIONS
- CONSTRUCTION AND TESTING OF EXPERIMENTAL MODEL TO VERIFY THEORETICAL MODEL

GEOMETRY OF THE REFLECTOR ANTENNA

The geometry of figure 1 is used to compute the radiation patterns of reflectors. The aperture integration technique is employed in obtaining these patterns: First, rays are traced from the feed to the reflector surface and then to an aperture plane located in front of the reflector. Next, using geometric optics for each ray, the tangential electric field is found at many points in the aperture plane and, by numerically performing a double integration over the aperture plane, the secondary far-field radiation pattern is computed. The relatively slow lateral variation of the fields in the aperture plane compared with that of the surface currents on the reflector allows a more economical computation than does the direct integration of surface currents.

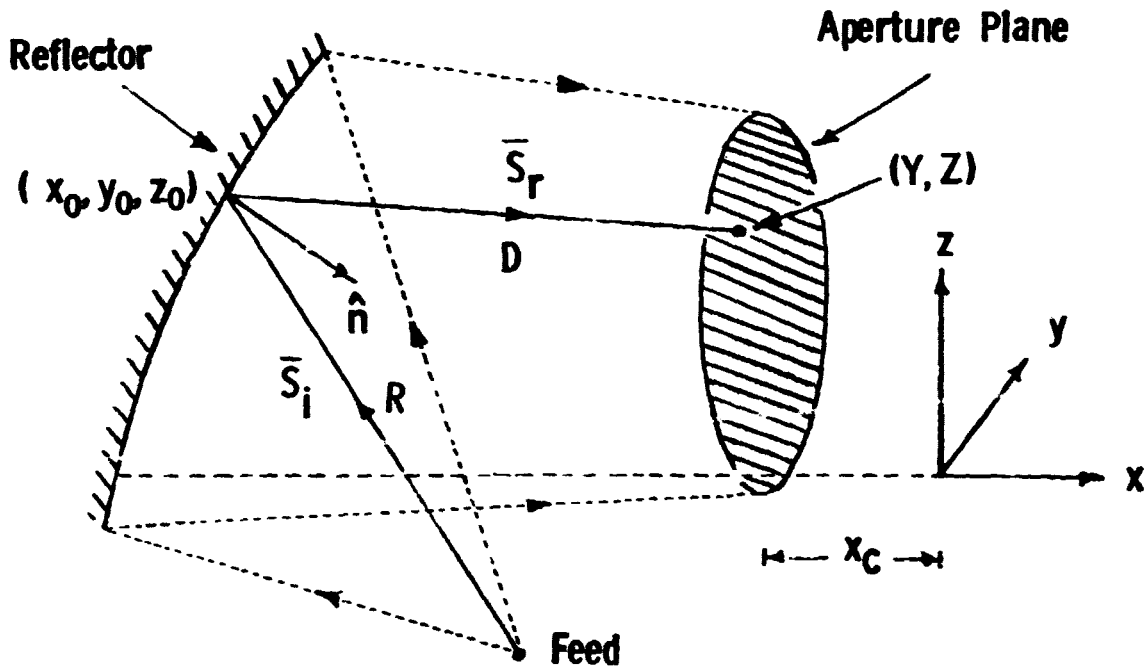


Figure 1

COMPUTED RADIATION PATTERNS FOR SEGMENTED
REFLECTORS USING APERTURE INTEGRATION METHOD

Shown in figure 2 are calculated H-plane radiation patterns for a spherical reflector which is approximated by a number of planar hexagonal, triangular, and square facets placed on the ideal sphere such that the RMS surface deviation in each case is the same (.012m). On the average the surface deviation is more slowly varying over the reflector approximated by planar hexagons than over that approximated by planar triangles. The pattern for the hexagonal approximation agrees better with the pattern for the exact spherical reflector (not shown). The pattern for the square approximation, however, has higher side lobes which are apparently caused by the regular surface deviation associated with this shape.

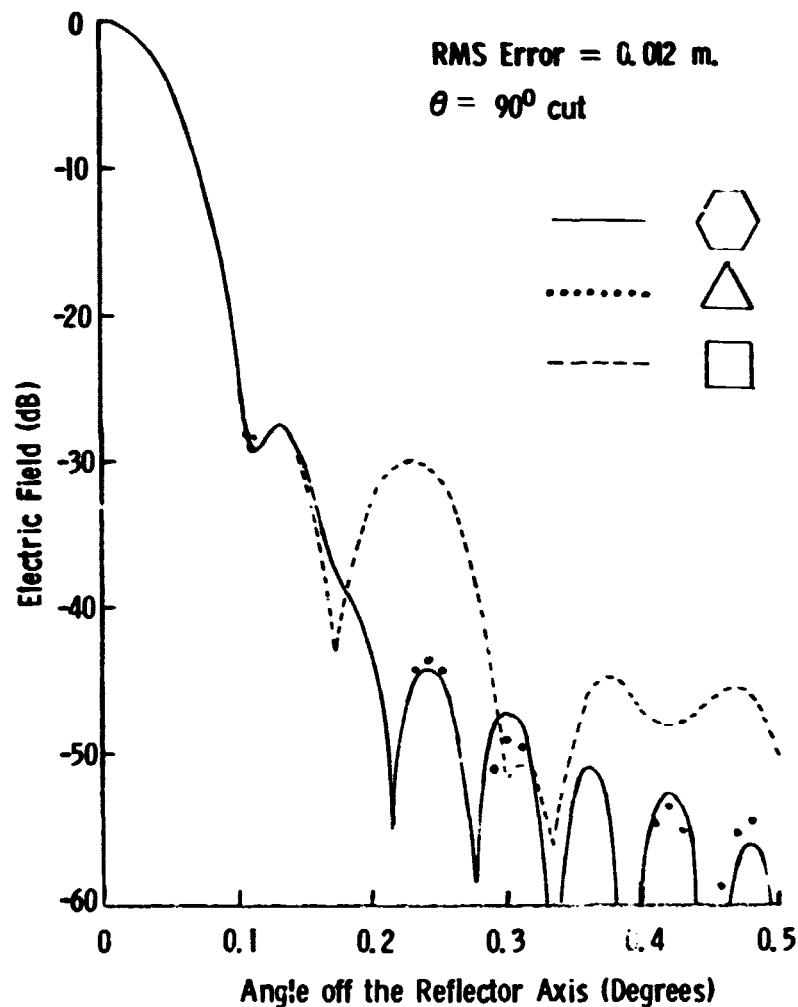


Figure 2

EFFECTS OF LARGE SCALE SURFACE ERRORS ON EM PERFORMANCE

An example of large scale deterministic type phase error (quadratic) effects on the radiation patterns of an aperture antenna is shown in figure 3. The solid curve corresponds to zero error ($\Delta=0$); i.e., the aperture distribution varies only in amplitude. The cases $\Delta=\lambda/8$ and $\Delta=\lambda/4$ correspond to increasing quadratic phase error with the same amplitude distribution. Increase in phase error results in an increase in power radiated in the side lobes.

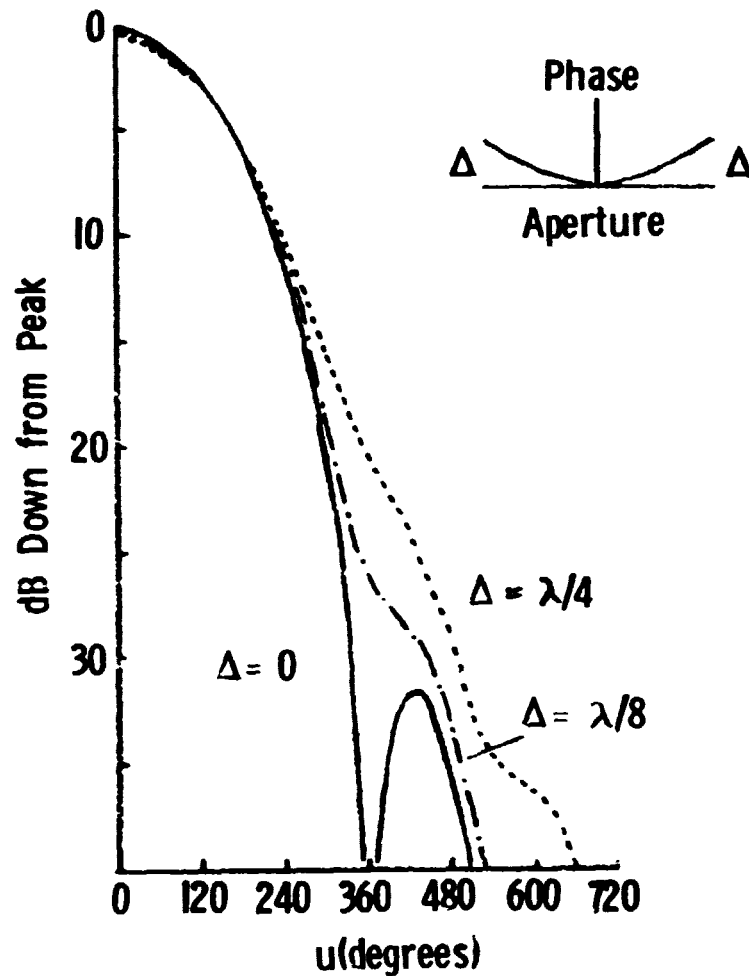


Figure 3

ENVELOPES OF RADIATION PATTERNS FOR
QUASI-RANDOM PHASE ERRORS

Figure 4 illustrates for a circular aperture antenna (diameter D) how the radiated power in the side lobes increases for a class of irregular phase errors (see inset) which may be characterized as quasi-random (ref. 1). The curve labeled 0 is error-free and the remaining curves represent indicated amounts of maximum peak to peak phase errors. Aperture tolerances corresponding to these phase errors are shown in the parentheses. The general effect of such irregular, but deterministic, phase errors is almost always to raise the side lobe levels and hence to lower the antenna beam efficiency.

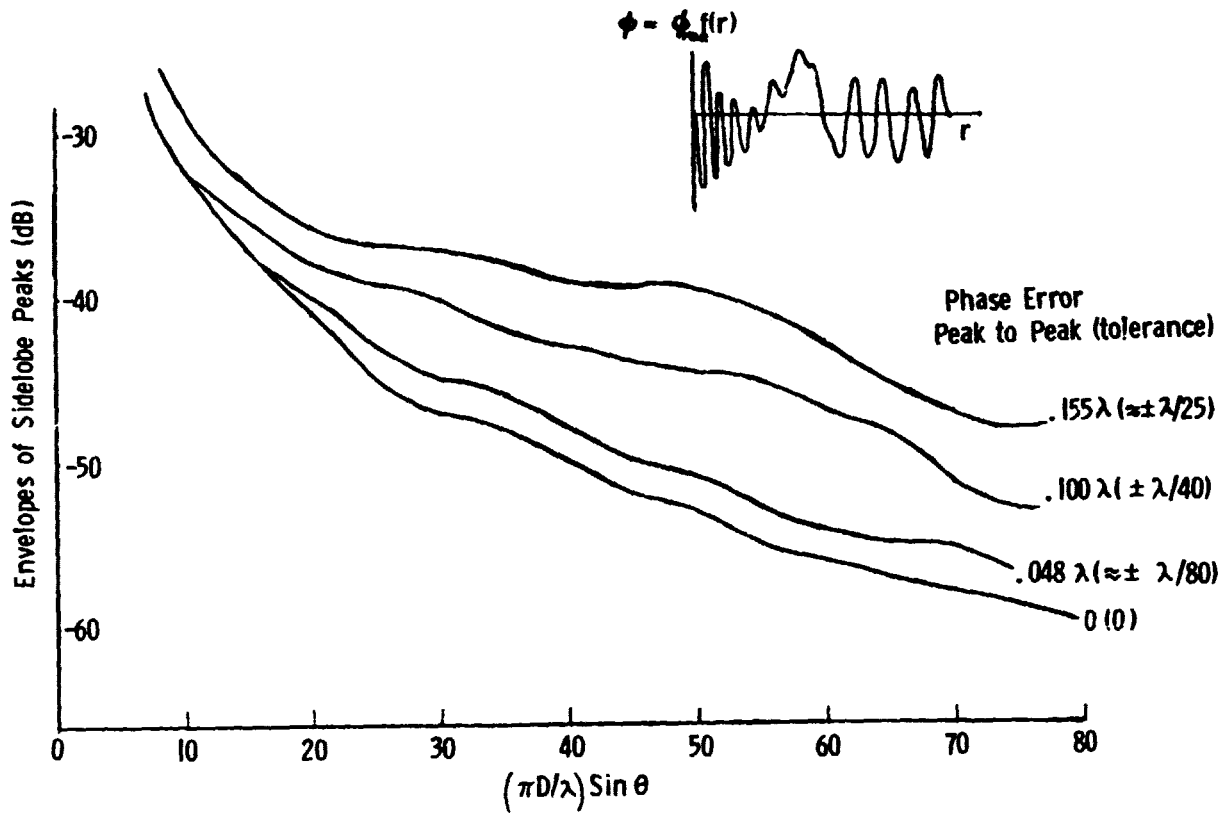


Figure 4

RADIATION PATTERNS OF 20-SEGMENT APERTURE
ANTENNA WITH GAUSSIAN DISTRIBUTED PHASE ERROR

Figure 5 shows the calculated radiation patterns of 20-segment aperture antennas of width D with assumption of uniform amplitude on all segments and Gaussian distributed phase error on each segment. The solid curve represents the radiation pattern when no phase error exists across the aperture. The dotted curve represents the expected (ensemble average) pattern which is obtained through random process analyses. The remaining radiation patterns come from two members of the ensemble of 20-segment aperture antennas.

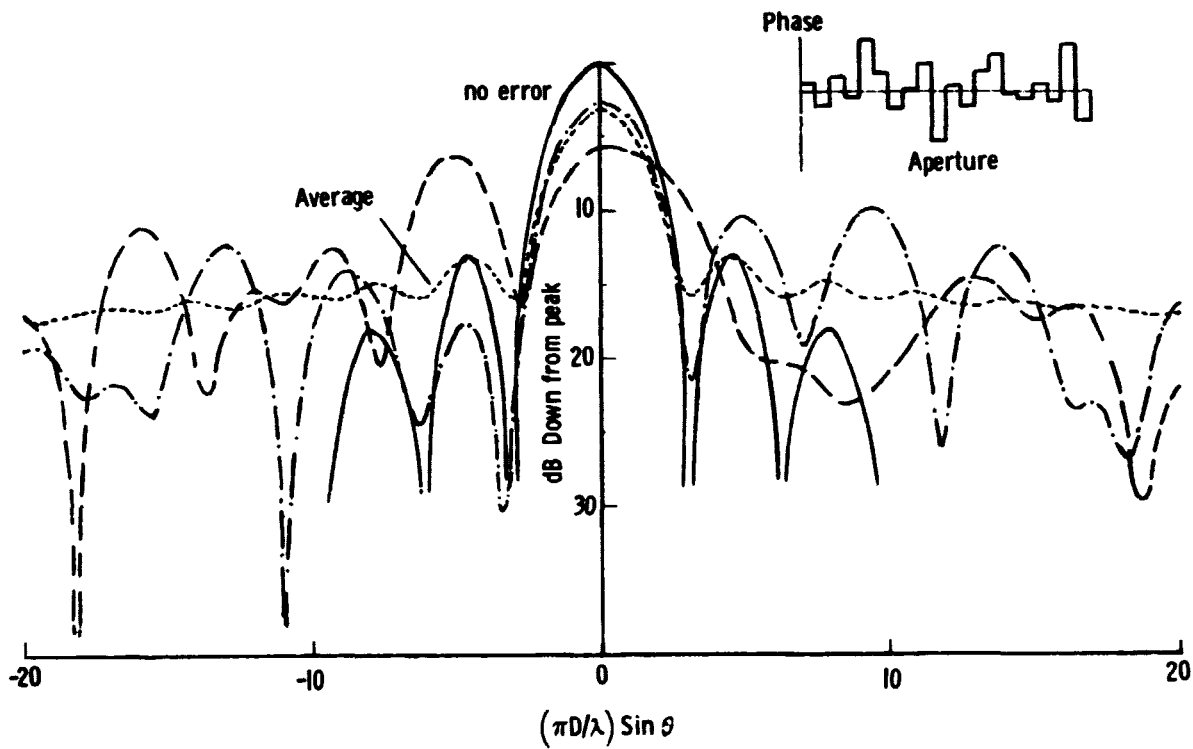


Figure 5

SECONDARY PATTERN BEAM EFFICIENCY vs. RMS
SURFACE ERROR IN WAVELENGTHS FOR DIFFERENT CORRELATION LENGTHS

The effects of surface errors on the beam efficiency of a large aperture antenna can be illustrated by applying the theory developed by Ruze (ref. 2). In Ruze's work the phase error (surface error) is chosen from a Gaussian population which is statistically uniform over the entire reflector surface. The auto-correlation function of the phase is also taken to have a Gaussian form with a constant variance (square of the correlation length). Based on his work the beam efficiency (assumed to be 100 percent for the unperturbed aperture) is plotted in figure 6 as a function of rms surface error with normalized correlation length (C/λ) as a parameter. It is seen that the smaller C/λ values (i.e., more rapidly varying surfaces) give rise to more stringent requirements on surface rms error for high beam efficiency. For more slowly varying surface (large C/λ) the surface rms error can be relaxed and still allow relatively high beam efficiency.

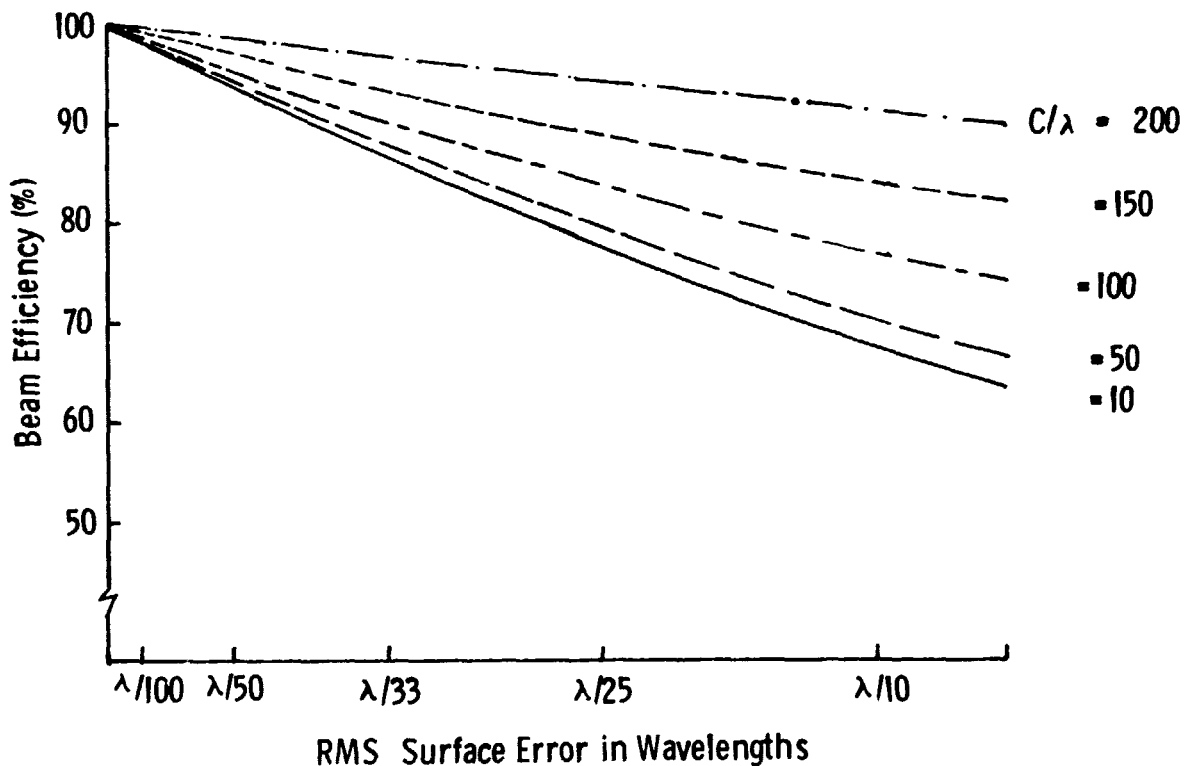


Figure 6

REAL PART OF THE AUTO-CORRELATION FUNCTION OF
20-SEGMENT APERTURE ANTENNA WITH
GAUSSIAN DISTRIBUTED PHASE ERROR

Figure 7 shows the real part of the auto-correlation function of a 20-segment aperture antenna with the assumption of uniform amplitude and Gaussian distributed phase error on each segment. The solid curve is the zero error case and the dotted curve is the ensemble average obtained through random process analyses. The two remaining curves are the real parts of the auto-correlation functions of two members of the ensemble of 20-segment aperture antenna. The Fourier transforms of the total auto-correlation functions (given in part in figure 7) are the power pattern curves given in figure 5.

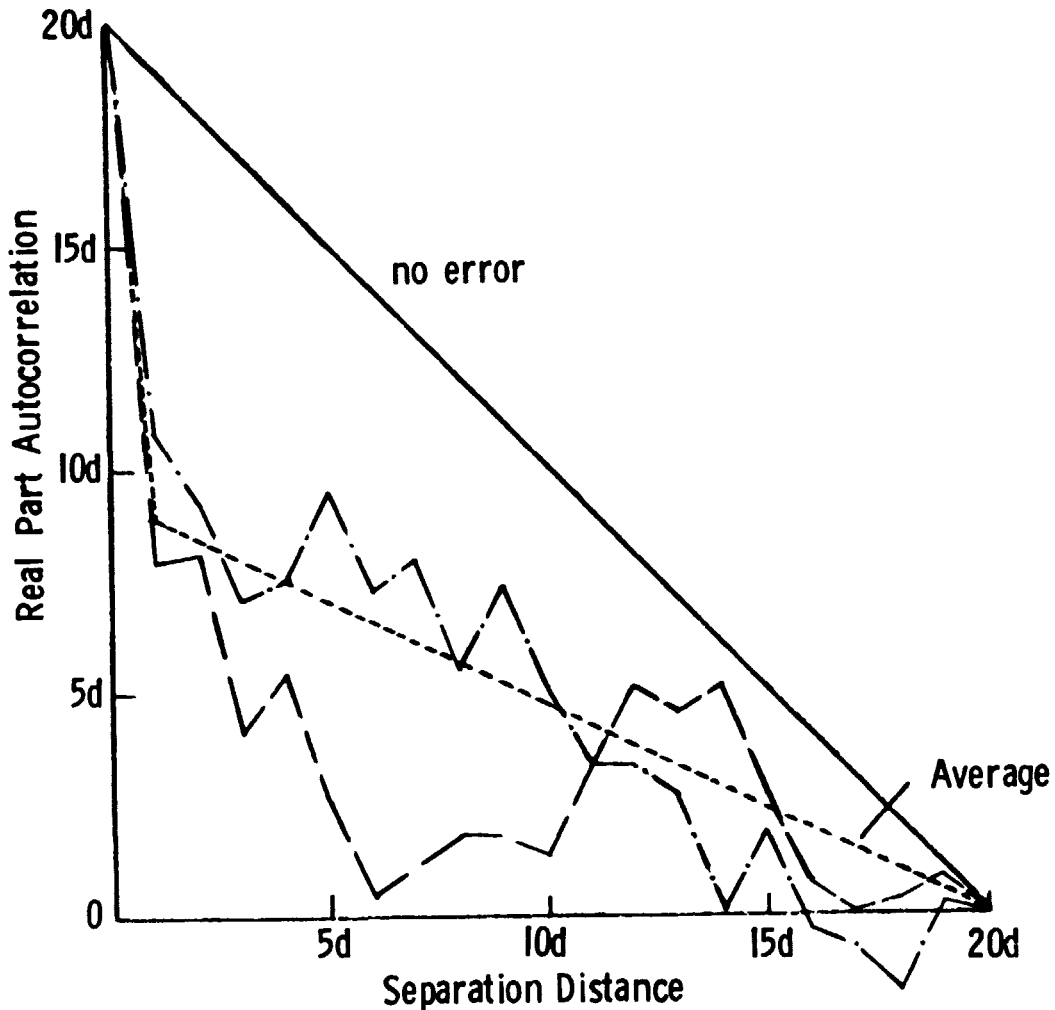


Figure 7

RATIOS OF STANDARD DEVIATION TO THE MEAN
AS A FUNCTION OF AUTO-CORRELATION SEPARATION DISTANCE

By observing figure 7, it can be seen that the auto-correlation functions from members of an ensemble of 20-segment aperture antennas can deviate from their ensemble average auto-correlation function (dotted curve in figure 7). The ratio of the standard deviation to mean for the 20-segment aperture antenna as a function of auto-correlation separation distance is given by the circles in figure 8. By increasing the number of segments within each antenna, the auto-correlation functions of the separate antennas approach arbitrarily close to the ensemble average (expected) auto-correlation function predicted by random process analyses. The increase in the number of segments clearly reduces the ratio of standard deviation to the means shown by the square and triangle symbols in figure 8.

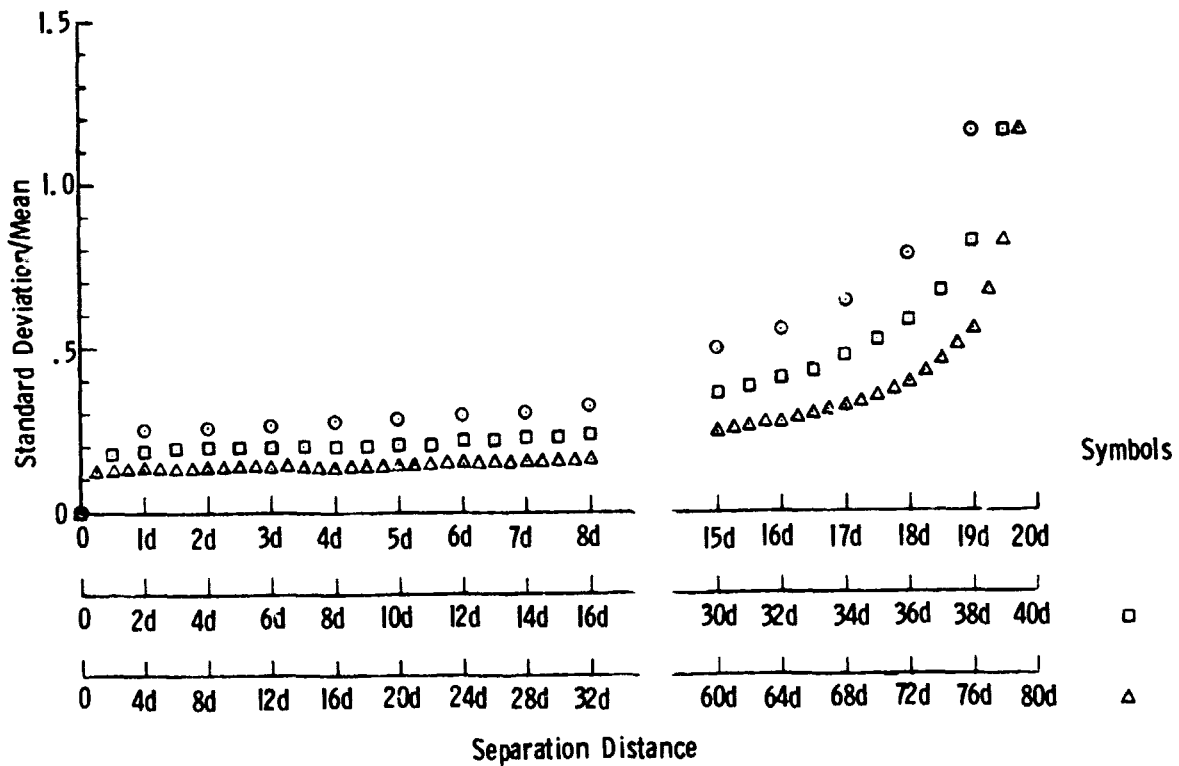


Figure 8

CONCLUDING REMARKS

- **Deterministic Analyses**
 - ◆ assumes exact knowledge of surface
 - ◆ true radiation patterns
 - ◆ both scale distortions
 - ◆ a range of possible distortions can lead to wide variance about the designed pattern

- **Random Process Analyses**
 - ◆ assumes statistical knowledge of surface
 - ◆ average radiation patterns
 - ◆ both scale distortions, provided correlation region is small compared to the aperture size
 - ◆ large correlation region can lead to large variance about the average pattern

- **General Effects of both Analyses**
 - ◆ broaden main beam
 - ◆ side lobe radiation increases with phase amplitude and variation
 - ◆ requirement of high beam efficiency in a very large antenna demands utmost care in EM analysis

C-3

PLANS FY '80

- EXPERIMENTALLY VERIFY SEGMENTED REFLECTOR PROGRAM
- EXPERIMENTALLY VERIFY SAMPLED POINT PROGRAM
- CONTINUE ANALYSES OF ANTENNAS THROUGH AUTOCORRELATION TECHNIQUES
- CONTINUE SEGMENTED REFLECTOR ANALYSES

PUBLICATIONS

- "A PRELIMINARY STUDY OF A VERY LARGE SPACE RADIOMETRIC ANTENNA," NASA TM 80047 , JAN. 1979, P.K. AGRAWAL
- "A METHOD FOR PATTERN CALCULATION FOR REFLECTOR ANTENNAS WHOSE GEOMETRY IS DESCRIBED BY A FINITE NUMBER OF DISCRETE SURFACE POINTS," IEEE APS SYMPOSIUM, JUNE 1979, P.K. AGRAWAL, J.F. KAUFFMAN, AND W.F. CROSWELL
- "PRELIMINARY DESIGN OF LARGE REFLECTORS WITH FLAT FACETS," NASA TM 80164, P.K. AGRAWAL, M.S. ANDERSON, M.F. CARD

REFERENCES

1. Dragone, C. and Hogg, D. C.: Wide-Angle Radiation Due to Rough Phase Fronts, Bell System Technical Journal, Vol. XLII, No. 5, September 1963.
2. Ruze, John: Antenna Tolerance Theory - A Review, Proc. IEEE, Vol. 54, pp. 633-640, April 1966.